

# The particle size distribution effect on the drying efficiency of polymeric fibers containing castables

Rafael Salomão, Victor C. Pandolfelli \*

*Federal University of São Carlos, Materials Engineering Department, Rod. Washington Luiz, Km 235 São Carlos, SP, Brazil*

Received 23 January 2006; received in revised form 5 February 2006; accepted 27 September 2006

Available online 13 November 2006

## Abstract

Refractory castables present several placing methods, defined mainly by the application requirements and material characteristics. Considering the same chemical composition, the particle size distribution (PSD) is the key property related to the large differences in their rheology, creep and corrosion resistance. It also plays an important role on their fluids permeation and drying behaviors. Therefore, it is reasonable to consider that the benefits promoted by polymeric fibers, added as drying agents, would be affected by PSD changes. In this work, the permeability and drying behaviors of fiber containing refractory castables were correlated to their PSD. Typical pumpable, self-flowing and vibrated formulations were tested in combination with polypropylene fibers. Permeability measurements and explosion tests were associated to the maximum paste thickness (MPT) and interparticle separation (IPS) parameters and to the fine/coarse particles ratio. The different classes of castables presented distinct needs of drying additives and the fibers' efficiency was strongly dependent on castables PSD.

© 2006 Elsevier Ltd and Techna Group S.r.l. All rights reserved.

**Keywords:** A. Drying; Refractory castables; Particle size distribution; Polymeric fibers

## 1. Introduction

Refractory castables are usually classified according to their placing method. Among them, the self-flowing, which are cast without external shearing; the pumpable, conveyed through pipes, and the vibrated ones [1–3]. For the same chemical composition, the particle size distribution (PSD) is usually the key property related to the differences in their rheological behavior [4,5] hot modulus of rupture, creep and corrosion resistance [3,6]. It also plays an important role in the permeation of fluids and, consequently, on the drying behavior of the castables [7–9].

Bearing in mind these differences, it is reasonable to consider that the benefits promoted by polymeric fibers added as drying promoters [10–16] would be also affected by the PSD changes. In this work, the permeability and drying behavior of fiber containing refractory castables were correlated to their PSD. Typical pumpable, self-flowing and vibrated refractory formulations were tested in combination with two different

polypropylene fibers. The results of permeability measurements, drying and explosion tests were associated to the maximum paste thickness (MPT) [17,18] and interparticle separation (IPS) parameters [4,5] and to the ratio between fine and coarse particles. It was verified that the different classes of castables tested presented distinct needs of drying additives and that the efficiency of the fibers was strongly dependent on the PSD of the castables.

### 1.1. PSD of castables and permeability

The studies recently carried out on refractory castables' permeability considered the high-alumina castables as two phase material, comprised of fine (diameter < 100  $\mu\text{m}$ , or matrix) and coarse (diameter  $\geq$  100  $\mu\text{m}$ , or aggregates) particles [7,9]. This criterion is based on the balance between the forces that actuate on suspension's particles: (a) the surface ones, that keep particles in suspension and prevail for particles smaller than 100  $\mu\text{m}$ , and (b) the gravitational ones, dominant for the coarser particles [1,19]. Several variables can affect this limit diameter such as solid load, shear rate and particles density, shape and interaction with the fluid and other particles, among others [19]. In the present work, this arbitrary limit was

\* Corresponding author.

E-mail addresses: [pers@iris.ufscar.br](mailto:pers@iris.ufscar.br), [vicpando@power.ufscar.br](mailto:vicpando@power.ufscar.br) (V.C. Pandolfelli).

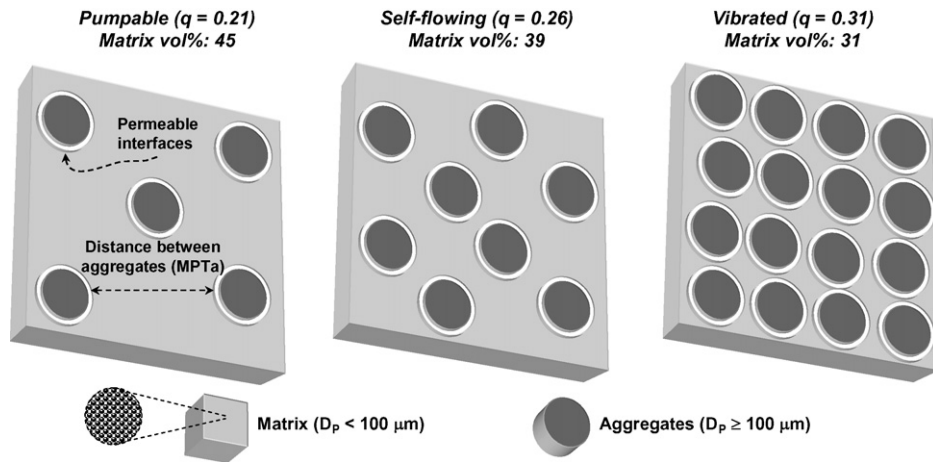


Fig. 1. Schematic view of the particle size distribution (PSD) in different classes of refractory castables.

kept in order to establish comparison with the results reported in literature, although the PSD as a whole defines the flow and packing behavior of the castables.

The flow of a permeant fluid through a fiber-free refractory castable structure can be carried out by two main permeable paths (Fig. 1). The first is the matrix–aggregate interfaces, generated by packing flaws due to the difference of particle size (*wall effect*) [7–9,20–22]. These regions, known as *interfacial transition zone* (ITZ) are porous, permeable and as thick as the finest particles. The number of matrix–aggregate interfaces can be estimated through the maximum paste thickness (MPT, Eq. (1)) parameter, which represents the distance between adjacent aggregates. Small MPT values in a castable formulation indicate that the coarse particles are close to each other due to the high coarse/fine particles ratio. As a consequence, the matrix–aggregate interface content scales with the permeable paths present in the castable.

The second and most important path for the permeant flow in refractory castables is through the porosity among the matrix particles [9]. As these permeable paths are thin and tortuous, the interparticle separation distance (IPS) plays an important role in the permeability and drying behavior of these materials, as recently reviewed [9]. Formulations with higher IPS values present a larger gap among matrix particles, allowing an easier flow of the permeant fluid through the structure of the castables.

The MPT [1,9,17,18] and the IPS [1,4,5,9] parameters can be calculated, respectively, by Eqs. (1) and (2).

$$\text{MPT} = \frac{2}{\text{VSA}_a} \left[ \frac{1}{\phi_a} - \left( \frac{1}{1 - P_{0,a}} \right) \right] \quad (1)$$

$$\text{IPS} = \frac{2}{\text{VSA}_m} \left[ \frac{1}{\phi_m} - \left( \frac{1}{1 - P_{0,m}} \right) \right] \quad (2)$$

VSA is the volumetric surface area ( $\text{m}^2/\text{cm}^3$ ),  $P_0$  the minimum theoretical packing porosity and  $\phi$  is the volumetric load of solids. Subscripts a and m indicate the parameters obtained for the aggregates and matrix paste fraction, respectively.

Compositions containing a high volumetric fraction of coarse particles present, simultaneously, smaller MPT values

and a larger gap between the matrix particles (greater IPS values). This kind of particle size distribution generates permeability values higher than those observed when a larger fraction of fine particles is employed. For the self-flowing, pumpable and vibrated refractory castables, typical percentage values of matrix/aggregate volumetric ratio are, respectively, 45–39%, 39–34% and 31–29% [1,2] and the differences in their permeability ( $k_2$ , measured using Forchheimer equation for compressible fluids) can be up to two orders of magnitude [7,8,12].

However, during the drying step of these materials, the permeability level provided by the ITZs and matrix porosity is usually not enough to release the vapor generated [9,14,16,23]. As a result of this mismatch between the amount of vapor generated and released, high pressure levels can be developed inside the structure. Depending on the heating schedule applied, water vapor pressure can rise quickly and attain the material's mechanical strength leading to explosive spalling. In order to prevent these explosions and mechanical damage, polymeric fibers are systematically added to the castable formulations [10–16].

## 1.2. Polymeric fibers as permeability enhancer for refractory castables

During their melting and thermal decomposition (starting at 165 °C, for polypropylene [14]) fibers contained in a refractory castable composition become soft and generate connections throughout the matrix and among the permeable matrix–aggregates interfaces [10,14]. This tri-dimensional net of paths allows an easier vapor release, reducing the internal pressure, increasing the drying rate and inhibiting the explosive spalling.

In order to effectively increase the permeability, the polymeric fibers must simultaneously fulfill two main requirements: (1) be added in a proper volumetric amount [16] and (2) present an adequate geometry to interconnect the ITZs and the channels that the fibers generated [12]. These conditions assure that, for a fixed amount of fibers added to the castable, the number of permeable interconnections that will be

formed in the structure and their efficiency will be maximized, as well as the permeability level attained.

The literature points out volumetric amounts close to 0.5% [11] and fiber diameters in the range of 8–20  $\mu\text{m}$  as the optimum condition to generate a great number of interconnections and a high permeability increase in pumpable castables [15]. For the same systems, the fiber length must be above 1 mm to enhance the permeability considerably [11–13,15]. These aspects are highly dependent on the particle size distribution of the castables and the distance among the ITZs, as will be seen later.

## 2. Materials and methods

### 2.1. Preparation of castables

The refractory castable composition was designed using the Andreasen particle packing model (Eq. (3)) [1]

$$\text{CPFT} = \left( \frac{D}{D_L} \right)^q \times 100 \quad (3)$$

where CPFT is the *cumulative percentage finer than* a specific particle diameter ( $D$ ),  $D_L$  the greatest particle diameter and  $q$  is the packing coefficient (the higher the  $q$  value, the more efficient the particle packing is). The formulations used the same raw materials (with the particle diameter varying from 0.1 to 4.750 mm) but with different  $q$  coefficients: pumpable ( $q = 0.21$ ), self-flowing ( $q = 0.26$ ) and vibrated ( $q = 0.31$ ).

The raw materials comprised a mix of fine matrix ( $D < 100 \mu\text{m}$ ), aggregates ( $D \geq 100 \mu\text{m}$ ), 2 wt% of calcium aluminate cement (CA14M, Almatiss US) and 4.5 wt% of water, used in particles homogenization and binder hydration. Citric acid was used as a dispersing agent in an amount of  $2.60 \times 10^{-4} \text{ mg/m}^2$  based on the castable surface area. In Table 1, the tested castable formulations are described in details. Polypropylene fibers of different lengths (1 mm and 3 mm long  $\times$  15  $\mu\text{m}$  of diameter) were added to a volumetric amount of 0.36% and dry mixed with the compositions (Table 2).

Mixing was carried out in a paddle mixer at a constant rotation (33 rpm). Water was added in a single step at a constant rate. After homogenization, compositions were vertically cast in cylindrical molds of 40 mm  $\times$  40 mm, for drying tests, and 25 mm long  $\times$  70 mm diameter, for permeability measurements. Samples were cured for 15 days in an acclimatized chamber (Vötsch 2020) at 8 °C in an atmosphere with a relative humidity close to 100%. The samples for drying evaluation were tested immediately after this period. Those prepared for permeability measurements were left another 96 h at 8 °C, under a relative humidity of 5% in order to remove the residual moisture.

### 2.2. Permeability measurements and drying tests

The permeability of the formulations was measured in green (dried at 8 °C and RU  $\approx$  5%) and fired (900 °C, for 6 h) samples. The Darcian ( $k_1$ ) and non-Darcian ( $k_2$ ) permeability

constants were calculated using the polynomial fitting of pressure and flow rate data of Forchheimer's equation (Eq. (4)) [24] expressed for compressible fluids as

$$\frac{P_i^2 - P_0^2}{2P_0L} = \frac{\mu}{k_1} V_s + \frac{\rho}{k_2} V_s^2 \quad (4)$$

where  $P_i$  and  $P_0$  are, respectively, the absolute air pressure at the entrance and exit of the sample,  $V_s$  the fluid velocity,  $L$  the sample's thickness, and  $\mu$  and  $\rho$  are, respectively, the viscosity and density of the fluid (air). The linear term of Forchheimer's equation ( $\mu V_s/k_1$ ), which represents the energy losses due to viscous friction, prevails at low fluid velocities. The quadratic term ( $\rho V_s^2/k_2$ ) denotes the contribution of inertia and turbulence on the pressure drop and is more relevant at higher fluid velocities. The values of the permeability constants, which may change significantly during the dewatering process, reflecting different microstructural phenomena, were obtained by fitting the experimental data of  $(P_i^2 - P_0^2)/2P_0L$  versus  $V_s$  in Eq. (2), using the least-square method [24].

The drying and spalling tests were performed in a thermogravimetric apparatus which allows for simultaneous recording of the mass variations and temperature profile inside the furnace and at the sample's surface [23]. Heating rates of 10 and 20 °C/min were applied, from 20 to 600 °C. The 10 °C/min heating rate shows the effects of the permeability of the material on the drying process more clearly and highlights the extension of each drying stage; the 20 °C/min one, better points out the explosive spalling resistance. The cumulative fraction of water lost during the heat-up ( $W$ , %), and the drying rate ( $dW/dt$ , % min $^{-1}$ ) were evaluated based on the following equations [23]

$$W(\%) = 100 \times \frac{M_0 - M}{M_0 - M_F} \quad (5)$$

$$\left( \frac{dW}{dt} \right)_i = \frac{W_{i+10} - W_{i-10}}{t_{i+10} - t_{i-10}} \quad (6)$$

where  $M$  is the instantaneous mass recorded at time  $t_i$  during the heating stages,  $M_0$  the initial mass, and  $M_F$  is the final mass of the tested sample.

## 3. Results and discussion

### 3.1. Permeability measurements

Fig. 2 states the permeability measurements carried out in fiber-free and polypropylene fiber containing castables formulations. Considering the green sample results, the huge differences among the permeability levels for the different compositions can be pointed out. As the PSD changes (from  $q = 0.21$  to  $q = 0.31$ ), more permeable ITZs are generated and the IPS increases, enhancing the permeability level of the castables [7,9,12]. The fiber addition did not affect the permeability of the green samples as before melting they do not provide paths to speed out water or water vapor release [11,14].

After thermal treatment, nevertheless, fiber addition promoted distinct permeability increases. In the pumpable

Table 1  
Tested formulations

Raw materials		Formulations		
		Pumpable ( $q = 0.21$ )	Self-flowing ( $q = 0.26$ )	Vibrated ( $q = 0.31$ )
<b>Matrix</b> (Diameter < 100 $\mu\text{m}$ , wt%)	Calcined aluminas and CA14M	18.20	20.10	14
<b>Aggregates</b> (Diameter $\geq 100 \mu\text{m}$ , wt%)	WEA* 200F	14.20	16.20	17.30
	WEA 40F	18.10	18.20	18.10
	WEA 20/40	9.00	7.00	10.00
	WEA 10/36	8.00	11.50	11.50
	WEA 08/20	9.00	9.00	11.10
	WEA 04/10	13.50	18.00	18.00
Parameters of the PSD employed		Formulations characteristics		
Surface area ( $\text{m}^2/\text{g}$ ) / VSA ( $\text{m}^2/\text{cm}^3$ )		1.67 / 7.10	1.16 / 6.52	0.81 / 5.72
Fraction of matrix (Diameter < 100 $\mu\text{m}$ , vol%)		45.00	39.00	31.00
Fraction of aggregates (Diameter $\geq 100 \mu\text{m}$ , vol%)		55.00	61.00	69.00
Interparticle separation distance (IPS, $\mu\text{m}$ )		0.039	0.048	0.061
Average maximum paste thickness (MPT, $\mu\text{m}$ )		79.96	84.56	90.26
Maximum paste thickness (calculated for aggregates > 500 $\mu\text{m}$ , MPTa, mm)		2.12	1.25	0.98
*WEA = white electrofused alumina				

Table 2  
Typical characteristics of the tested polypropylene fibers

Composition	Polypropylene (PP)
Density ( $\text{g}/\text{cm}^3$ )	0.91 $\text{g}/\text{cm}^3$
Melting point ( $^{\circ}\text{C}$ )	165
Nominal [and measured after mixing] lengths (mm)	1 [ $1.75 \pm 0.15$ ] and 3 [ $3.33 \pm 0.45$ ]
Diameter ( $\mu\text{m}$ )	$15 \pm 0.1$
Amount (vol%)[wt%]	0.36 [0.1]

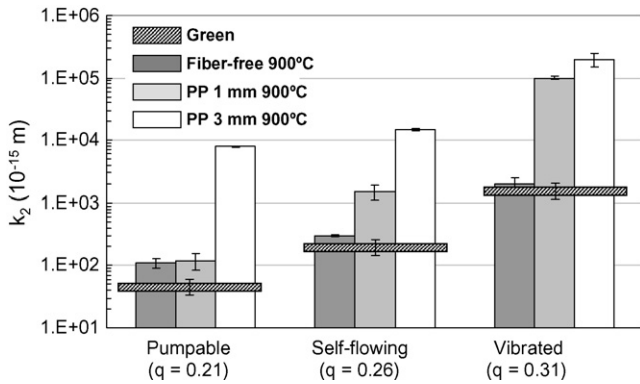


Fig. 2. Combined effect of PSD and fiber length on castables permeability ( $k_2$ ).

castable, the permeability increase was observed only for the 3 mm long fiber containing compositions. For the self-flowing and the vibrated compositions, both fiber lengths generated a permeability increase. This difference in the minimum fiber length required to promote the permeability increase can be related to the distance among the ITZs and the other fibers. The MPT parameter was used in order to estimate this relationship.

For the high-alumina castables tested in the present work and in several other systems in the literature (also with particle size varying from 1  $\mu\text{m}$  to 4.750 mm, containing 15 vol% of water), MPT typical values are about 80–90  $\mu\text{m}$  (Table 1) [3,9]. These values indicate that the average distance among the ITZs is much smaller than the fiber length, which does not match the experimental results of Fig. 2 (i.e.  $q = 0.21$ ). However, it is important to observe that this average value was obtained considering aggregates with sizes varying from 100  $\mu\text{m}$  to 4.750 mm. If only the coarsest fraction of the aggregates (diameter > 0.5 mm) were considered in the MPT evaluation, the  $VSA_a$  and  $\Phi_a$  parameters would be drastically reduced and the dimension of the MPT value would increase from 79.96  $\mu\text{m}$  to 2.12 mm, for the pumpable castables, for example.

This higher MPT value could be understood as an indication of the distance among the highest permeable ( $MPT_a$ ) and less tortuous interfaces or, in other words, the minimum fiber length needed to interconnect them. The  $MPT_a$  represents the

maximum fiber length above which is much more likely to the fibers to touch themselves. Consequently, the interconnection and permeability increase only occur when fiber length is similar or greater than the  $MPT_a$ , as seen for the self-flowing and vibrated compositions. Nevertheless, if fibers shorter than the  $MPT_a$  are used, as the 1 mm fibers in the pumpable castable, the connections generated present low efficiency and behave as close pores.

The  $MPT_a$  values presented in Table 1 demonstrate that, when the distance among the matrix–aggregate interface of the coarsest aggregates is reduced, fibers with shorter lengths are able to promote the permeability increase (Fig. 3) by the interconnection of the ITZs and the paths left after the fibers melt and degradation. It can be also noted that the longer the fiber length after mixing, the higher the level of permeability attained is. This aspect was already described elsewhere and indicates that longer fibers present better efficiency to interconnect more permeable paths at the same time [11,12].

### 3.2. Drying and explosion tests

The results of drying and explosion tests for the different castables compositions are shown in Figs. 4–7. The drying behavior of refractory castables can be generally described as being composed of three main stages, identified as three main peaks in the drying rate versus time curves [23]. The first represents the water withdrawal during the evaporation stage (below 100 °C). It is carried out under a low drying rate and with almost no pressurization in the structure. The second, which is the ebullition (100–300 °C), presents the higher drying rate and explosion risks, since water is released as pressurized vapor. After these stages, only the water, which is chemically bonded, remains in the structure. Depending on the hydraulic binder used, this step can reach high temperatures (up to 400 °C), but due to the smaller amount of water present typically in a 2 wt% cement containing castable, the risks of explosion are reduced.

The tests conducted at 10 °C/min on the fiber-free samples revealed the remarkable effect of the permeability of castables on their drying behavior. The pumpable composition, with the

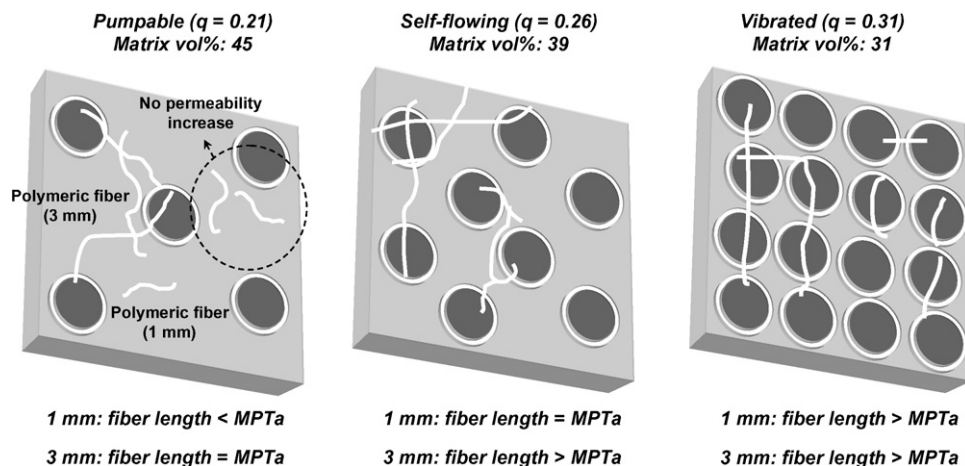


Fig. 3. Effect of different length polymeric fiber addition to castables with distinct PSD.

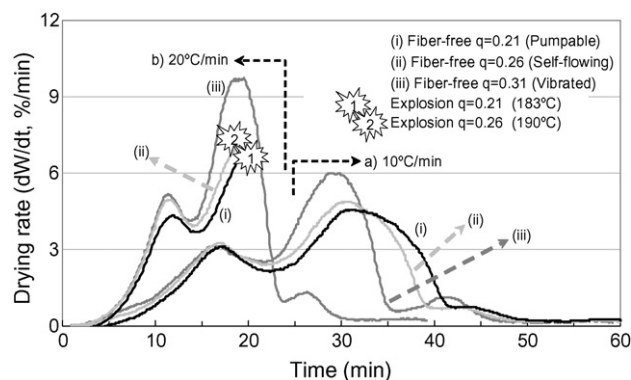


Fig. 4. Drying tests for fiber-free castables formulated with different PSD (at heating rates of 10 and 20 °C/min).

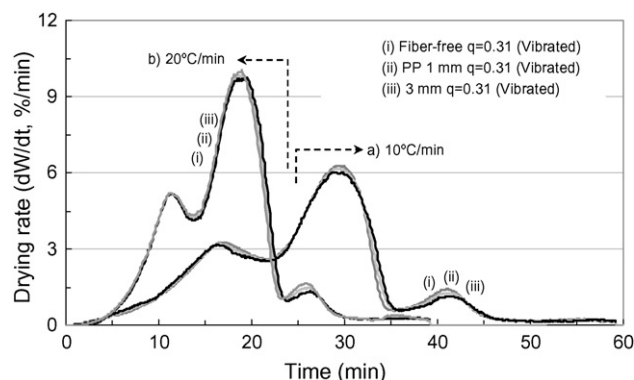


Fig. 7. Drying tests for vibrated castables ( $q = 0.31$ ) containing polypropylene fibers of different lengths (at heating rates of 10 and 20 °C/min).

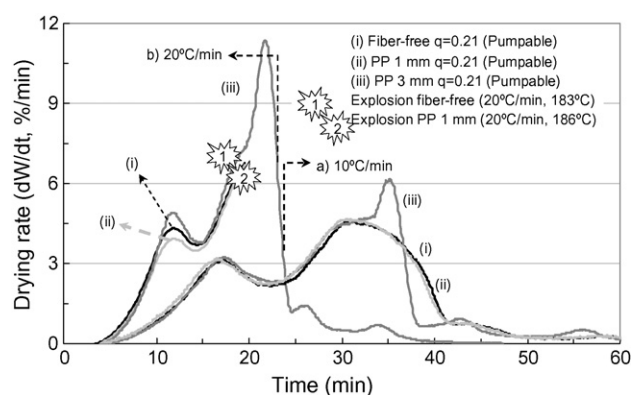


Fig. 5. Drying tests for pumpable castables ( $q = 0.21$ ) containing polypropylene fibers of different lengths (at heating rates of 10 and 20 °C/min).

lowest permeability, presented a smaller drying rate and a longer drying time. The vibrated one, on the other hand, showed a greater drying rate and a smaller drying time. The self-flowing castable showed an intermediate behavior. When a higher heating rate was used (20 °C/min), the pumpable and the self-flowing formulations exploded, whereas the vibrated remained up to the end of the drying. Therefore, for the systems studied, if a minimum permeability level is achieved by PSD modifications, the explosion can be inhibited, even without the use of drying additives, as observed for the vibrated composition.

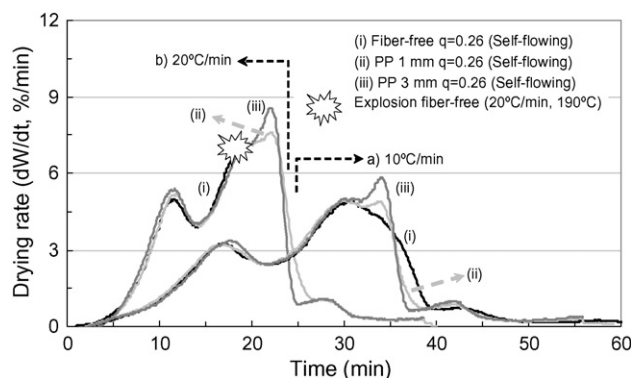


Fig. 6. Drying tests for self-flowing castables ( $q = 0.26$ ) containing polypropylene fibers of different lengths (at heating rates of 10 and 20 °C/min).

These results are compatible with the literature and with the permeability measurements carried out [6,9].

As the benefits of polymeric fibers as drying additives is based on the permeability increase, the higher the magnitude of the permeability increase attained, the greater the drying rate. On the other hand, if the fiber addition did not affect the permeability of a particular castable formulation, it will not bring benefits to the drying step [14,16]. This statement can be strengthened by the results presented in Figs. 5–7 where the fiber addition led to distinct changes on the drying behavior of the various castable compositions.

The 1 mm fibers did not affect the drying of the pumpable composition, because they were not able to promote a permeability increase. However, for the self-flowing composition, they were effective in enhancing the drying rate and inhibiting the explosion. The 3 mm ones, on the other hand, promoted the higher permeability increase in both formulation and, due to this, their effect was more significant than the 1 mm ones, as an explosion was avoided and the drying rate was highly increased. For the vibrated composition, a different behavior was observed and fibers presented a small effect. This result was not caused by the lack of permeability increase in the fiber containing samples, but due to its intrinsic high permeability based on the PSD. As the water vapor did not face difficulties to be released, the increase in  $k_2$  value almost did not affect the drying rate.

The permeability measurements and the results of drying and explosion tests suggested that the classes of refractory castables studied require different drying additive designs to reduce the risks of explosive spalling. They are directly related to the particle size distribution used in the castable formulation and the correspondent permeability level generated. Low permeability castables (such as the pumpables and self-flowing) require a great permeability increase to reduce the internal water vapor pressure. In such cases, fibers must be carefully selected in order to suit the PSD and generate effective permeable interconnections. For the more permeable ones (vibrated), smaller enhancements in the permeability levels are sufficient as the vapor pressure generated is lower. A summarized view of these aspects is shown in Table 3.

Table 3

Effects in drying generated by the polymeric fiber addition in different PSD refractory castables formulations

<b>Pumpable (<math>q = 0.21</math>)</b>	<b>Self-flowing (<math>q = 0.26</math>)</b>	<b>Vibrated (<math>q = 0.31</math>)</b>
<b>Fiber-free and 1 mm fiber containing:</b> <ul style="list-style-type: none"> <li>• Explosion at the 20°C/min heating rate</li> <li>• Low permeability castable and no permeability increase was verified</li> <li>• No suitable drying additive</li> </ul>	<b>Fiber-free:</b> <ul style="list-style-type: none"> <li>• Explosion at the 20°C/min heating rate</li> <li>• Low permeability castable and no permeability increase occurred</li> <li>• No drying additive</li> </ul>	<b>Fiber-free:</b> <ul style="list-style-type: none"> <li>• No explosion at the 20°C/min heating rate</li> <li>• Intrinsically high permeability castable</li> <li>• No need of drying additive</li> </ul>
	<b>1 mm fiber containing:</b> <ul style="list-style-type: none"> <li>• No explosion at the 20°C/min heating rate</li> <li>• Low permeability castable but permeability increase was verified</li> <li>• Effective drying additive</li> </ul>	<b>1mm and 3mm fiber containing:</b> <ul style="list-style-type: none"> <li>• No explosion at the 20°C/min heating rate</li> <li>• High permeability castable and permeability increase               <ul style="list-style-type: none"> <li>• Drying additives did not affected in a significant way the drying rate</li> </ul> </li> <li>• Nevertheless, they would help if necessary</li> </ul>
<b>3 mm fiber containing: no explosion:</b> <ul style="list-style-type: none"> <li>• No explosion at the 20°C/min heating rate</li> <li>• Low permeability castable but permeability increase was verified</li> <li>• Effective drying additive</li> </ul>	<b>3 mm fiber containing: no explosion:</b> <ul style="list-style-type: none"> <li>• No explosion at the 20°C/min heating rate</li> <li>• Low permeability castable but permeability increase was verified</li> <li>• Effective drying additive</li> </ul>	

The fact that short fibers (<3 mm) can be used as drying additives in certain classes of castables has another important consequence for the other steps of processing these materials. The addition of fibers can increase the energy required for mixing and reduce the flowability of the castables [13,25]. These effects scale with fiber length, due to the particles bridging promoted by them. Therefore, replacing the fibers commonly used (3–6 mm) by shorter ones (1 mm), reduces the mixing and flow side effects without affecting the drying benefits.

#### 4. Concluding remarks

Polypropylene fibers can bring benefits such as drying additives in all the classes of refractory castables tested. Their effective performance depends on a suitable match between fiber geometry and the castable particle size distribution. As fiber actuation mechanism is based on the permeability increase, when it does not occur, no benefits in drying are observed. Due to the larger distance between the matrix–aggregates permeable interfaces, the pumpable castable required fibers with lengths greater than 1 mm in order to promote permeability increase and avoid explosion. Due to their higher aggregate/matrix ratio, the self-flowing composition presents a shorter distance among these interfaces and due to this shorter fibers were able to provide permeability and a drying rate increase, as well as to inhibit the explosion. For the

vibrated composition, although all fibers promoted a considerable permeability increase, no significant benefits in the drying were observed. Differently from the pumpable composition, in this case, its intrinsic high permeability as a result of PSD, made water vapor so easy to be released that the permeability increase generated by the fibers was not as useful.

#### Acknowledgments

The authors are grateful to the Brazilian Research Funding, FAPESP, to ALCOA S.A. (Brazil) and MAGNESITA S.A. (Brazil) for supporting this work.

#### References

- [1] I.R. Oliveira, A.R. Studart, R.G. Pileggi, V.C. Pandolfelli, Dispersion and Packing of Particles—Basic Principles and Applications to Ceramic Processing (in Portuguese), Fazenda Arte Editorial, Brazil, 2000, p. 195.
- [2] R.G. Pileggi, V.C. Pandolfelli, Rheology and particle size distribution of pumpable refractory castables, *Am. Ceram. Soc. Bull.* 80 (10) (2001) 52–57.
- [3] A.R. Studart, R.G. Pileggi, J. Gallo, V.C. Pandolfelli, High-alumina multifunctional refractory castables, *Am. Ceram. Soc. Bull.* 80 (11) (2001) 34–40.
- [4] J.E. Funk, D.R. Dinger, Predictive Process Control of Crowded Particle Suspensions Applied to Ceramics Manufacturing, Kluwer Academic Publishers, England, 1994.
- [5] J.E. Funk, D.R. Dinger, Particle size control for high-solids castables refractories, *Am. Ceram. Soc. Bull.* 73 (10) (1994) 66–69.

- [6] R.G. Pileggi, A.R. Studart, M.D.M. Innocentini, V.C. Pandolfelli, High-performance refractory castables, *Am. Ceram. Soc. Bull.* 81 (6) (2002) 37–42.
- [7] M.D.M. Innocentini, A.R. Studart, R.G. Pileggi, V.C. Pandolfelli, How PSD affects the permeability of refractory castables, *Am. Ceram. Soc. Bull.* 80 (5) (2001) 31–36.
- [8] M.D.M. Innocentini, C. Ribeiro, J. Yamamoto, A.E.M. Paiva, L.R.M. Bittencourt, R.P. Rettore, V.C. Pandolfelli, Drying behavior of refractory castables, *Am. Ceram. Soc. Bull.* 80 (11) (2001) 47–56.
- [9] M.D.M. Innocentini, R.G. Pileggi, F.T. Ramal Jr., V.C. Pandolfelli, PSD-designed refractory castables, *Am. Ceram. Soc. Bull.* 82 (7) (2003) 1–6.
- [10] D.P. Bentz, Fibers, percolation and spalling of high-performance concrete, *Am. Conc. Inst. Mat. J.* 97 (3) (2000) 351–359.
- [11] R. Salomão, F.A. Cardoso, M.D.M. Innocentini, L.R.M. Bittencourt, V.C. Pandolfelli, Effect of polymeric fibers on refractory castables permeability, *Am. Ceram. Soc. Bull.* 82 (4) (2003) 51–56.
- [12] R. Salomão, C.S. Isaac, F.A. Cardoso, M.D.M. Innocentini, V.C. Pandolfelli, PSD, polymeric fibers and the permeability of refractory castables, *Am. Ceram. Soc. Bull.* 82 (10) (2003) 931–935.
- [13] R. Salomão, V.G. Domiciano, C.S. Isaac, R.G. Pileggi, V.C. Pandolfelli, Mixing step and permeability of polymeric fiber-containing refractory castables, *Am. Ceram. Soc. Bull.* 83 (1) (2004) 9301–9308.
- [14] R. Salomão, V.C. Pandolfelli, Drying behavior of polymeric fiber-containing refractory castables, *J. Tech. Assoc. Refract. Jpn.* 24 (2) (2004) 83–87.
- [15] R. Salomão, A.M. Zambon, V.C. Pandolfelli, Polymeric fibers geometry affects refractory castables permeability, *Am. Ceram. Soc. Bull.* 85 (4) (2006) 9201–9205.
- [16] R. Salomão, V.C. Pandolfelli, A systemic view of the effect of fibers on processing refractory castables, *J. Eur. Ceram. Soc.*, submitted for publication.
- [17] T.C. Powers, *The Properties of Fresh Concrete*, John Wiley & Sons, Inc., USA, 1968, p. 664.
- [18] P. Bonadia, A.R. Studart, R.G. Pileggi, S.L. Vendrasco, V.C. Pandolfelli, Applying MPT principle to high-alumina castables, *Am. Ceram. Soc. Bull.* 78 (3) (1999) 57–60.
- [19] R. Darby, Hydrodynamics of slurries and suspensions, in: N.P. Cheremisinoff (Ed.), *Encyclopedia of Fluid Mechanics: Slurry Flow Technology*, Gulf Publishing, USA, 1986, pp. 49–91.
- [20] J.P. Ollivier, J.C. Maso, B. Bourdette, Interfacial transition zone in concrete, *Adv. Cem. Bas. Mat.* 2 (1995) 30–38.
- [21] K.L. Scrivener, K.M. Nemati, The percolation of pore space in the cement past/aggregate interfacial zone of concrete, *Cem. Concr. Res.* 26 (11) (1996) 35–40.
- [22] E.J. Garboczi, D.P. Bentz, Analytical formulas for interfacial transition zone properties, *Adv. Cem. Bas. Mat.* 6 (1997) 99–108.
- [23] M.D.M. Innocentini, F.A. Cardoso, M.M. Akyioshy, V.C. Pandolfelli, Drying behavior of refractory castables, *J. Am. Ceram. Soc.* 86 (7) (2003) 1146–1148.
- [24] M.D.M. Innocentini, A.R.F. Pardo, V.C. Pandolfelli, Permeability of high-alumina refractory castables based on various hydraulic binders, *J. Am. Ceram. Soc.* 85 (6) (2002) 1517–1521.
- [25] R. Salomão, V.G. Domiciano, V.C. Pandolfelli, Rheological behavior of polymeric fibers containing refractory castables, *Am. Ceram. Soc. Bull.* 85 (5) (2006) 21–24.